

## Geophysical Interpretation

Processing and interpretation for all geophysical survey types have been performed in Geoplot, Surfer, RADAN and ArcGIS. Data were processed in appropriate software, examined for archaeological features and input to ArcGIS. Each anomaly identified in the data is digitised as a point, line, or polygon shape. Each anomaly has an x, y position corresponding to Ordnance Survey (OS) map coordinates and an assigned attribute value defining its' interpreted character.

All interpretations are based on the author's knowledge of geophysical survey methods, expected results, and site specific archaeology and geology. All interpretation images are paired with a blank data image. Site archaeological experts should study data results, as they may be able to better recognise archaeological and non-archaeological anomalies. Images supplied in this should be adequate for initial review, but a thorough review of data to exhaust all possible information would best be conducted with geophysical survey experts and site experts.

Factors that contribute to background noise in data in the Focus area include: modern farming activity, past land use, a prolific rabbit population, changes in weather (ground saturation), a possible changing water table (due to continuous gravel extraction adjacent to site), and underlying geology.

All data are displayed with a greyscale legend, values are white – low to black – high.

### *Ground Penetrating Radar:*

GPR data were collected over approximately 3.5 hectares with a SIR3000 radar system using a 400 MHz antenna with a survey wheel. Data were collected at a rate of 70 scans per meter, regulated by the survey wheel. Data collection set-ups were performed in the field to best capture the most information possible. Knowing that the archaeological targets to be mapped were assumed to be no more than 1 m from the ground surface, a time window of 70 ns was set. This setting targets an expected depth of approximately 2 m for a material with the dielectric permittivity of 30 (an approximated value for the gravely, sandy soil of the survey area established through migration of various hyperbolas in data across the site.)

Issues of gain are discussed above in the GPR methods section. The only problem encountered with data collection during this process was the ability to match the gain properties across grids. 4 gain points were set to enhance the signal as it passes into the ground (and loses energy). These points were set carefully in order to best represent the information in the ground. Due to equipment limitations (the SIR 3000 is the newest model system from Geophysical Survey Systems, Inc. (GSSI) the machine used on this project was one of the first released and contained some initial system bugs), data collection was limited to a maximum of 10 files before having to be downloaded to a laptop in the field (or the system would crash). As a result, every 10 m in Field F the gain varies slightly and can be seen in the surface time slices in the GIS. The only way around this is to collect data without any gain in the field, virtually "blind", meaning that subsurface anomalies would not be visible to the technician. The gain effects are not as prominent in fields B and A. New hardware

upgrades have eliminated this problem. The remaining issue with gain will exist on a more day to day basis as site properties will continue to change (soil saturation).

All GPR data are displayed with ns as the vertical axis (z component). The actual depth of each slice (and subsequently, identified anomalies) can be estimated, but only through excavation can they be made absolute. Individual GPR profiles are displayed in ns with the 3D cube working in ns mode for the vertical axis (choice of meters, ns, or samples). The time slices (or horizontal plan views of interpolated profiles) that are used in the GIS range between 5 and 8 ns thick. This measurement was determined through close examination of the data and determined to be best suited to displaying the archaeology and other anomalies of interest.

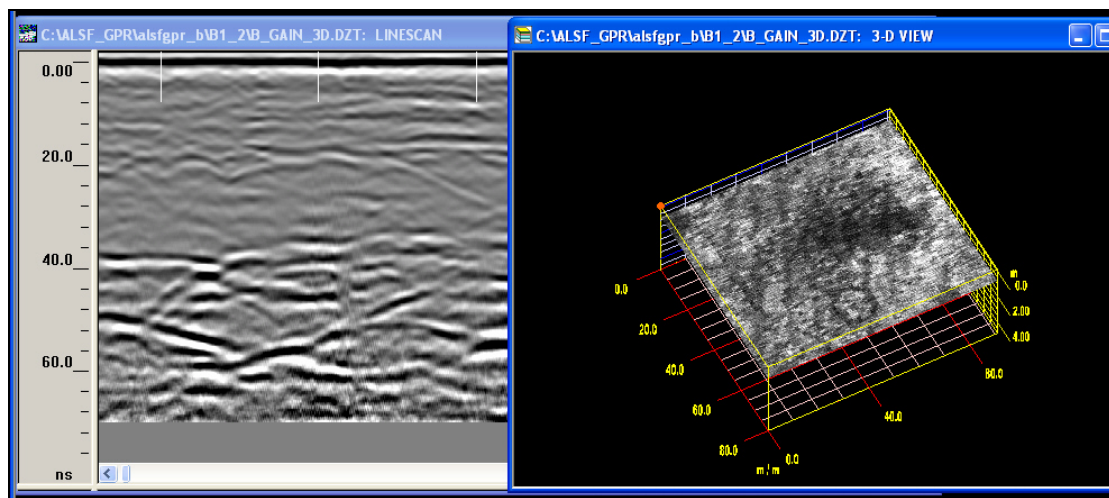


**Figure 18** GPR vertical profile and 3D cube. Note the vertical profile is measured in ns.

Once imaged in time slices, Field B had slices extracted for input to the GIS at levels that best displayed the character of the earth at that time. Fields A and F have been sampled at 5 ns intervals beginning at the ground surface, or 0 ns. Field F has additional time slices extracted that best display the character of the archaeology.

Analysis has been performed in both the GIS and in RADAN (GSSI's dedicated GPR processing and imaging program.) Review of data in both programs has led to the most effective interpretation possible.

All interpretations have been recorded to reflect possible archaeological anomalies. Modern ploughing effects have not been recorded, nor have possible ridge and furrow ploughing traces been mapped. Possible ridge and furrow features exist in fields A, B, and F and are best mapped with the GPR. Examples of the possible ridge and furrow will be shown in the sections on GPR interpretations for fields B and F.

GPR interpretations are targeting what can be best categorized as possible archaeology. Geological features have not been interpreted (though some features will be shown in sections of the GPR interpretations for fields B and F.) Some factors that must be kept in mind during data processing include: modern occupation effects and past fluvial activity, to name a few.

- Modern occupation of this site includes activity from farming that is evident in very strong plough furrow lines in the data. In addition to these

lines one must consider the effects of ploughing for decades on the site, ploughing in different directions may cause the high concentration of gravels in the soil to collect in concentrated groups. This will appear as a strong amplitude reflector in the data.

- Past fluvial activity in this area will have deposited gravels and sands across the site (this can be seen clearly in the deeper region of the GPR data). Though some of this activity can be recognized in larger data patterning trends, some of the reflectors that will appear in the data may be irregular remainders of materials deposited from fluvial activities.

*Field A:*

A 60 x 100 m grid of data was collected in Field A. This grid was established with coverage of a good part of the 'woodhenge' monument according to the mapped crop marks, and a region to the west with no apparent anomalies.

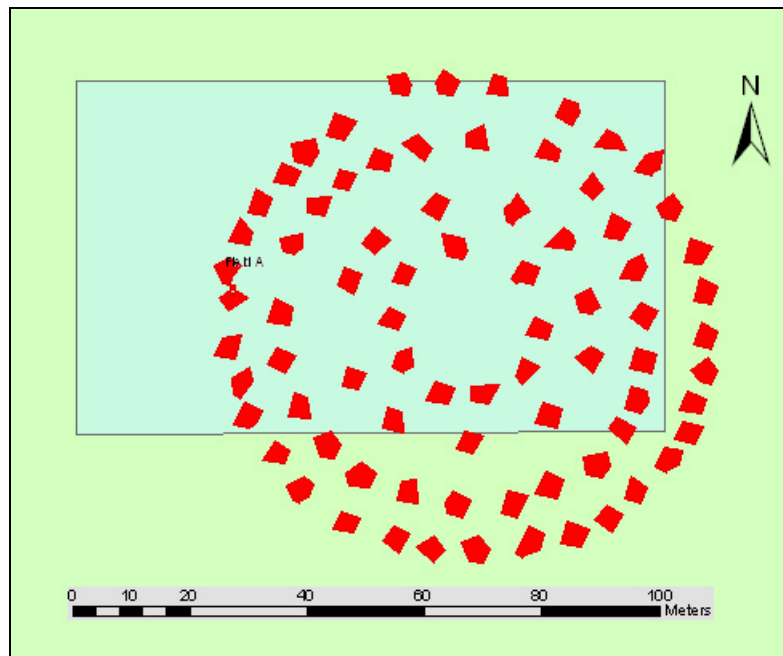


**Figure 19 Field A GPR survey grid.**

The GPR data from Field A show a few areas of high amplitude reflection. These anomalies have been selected because of their basic shape and amplitude. A few linear anomalies have also been recorded, the one passing through the grid from west to east, is probably a deeper plough furrow from previous farming activities (in this case, it is probably ridge and furrow.)

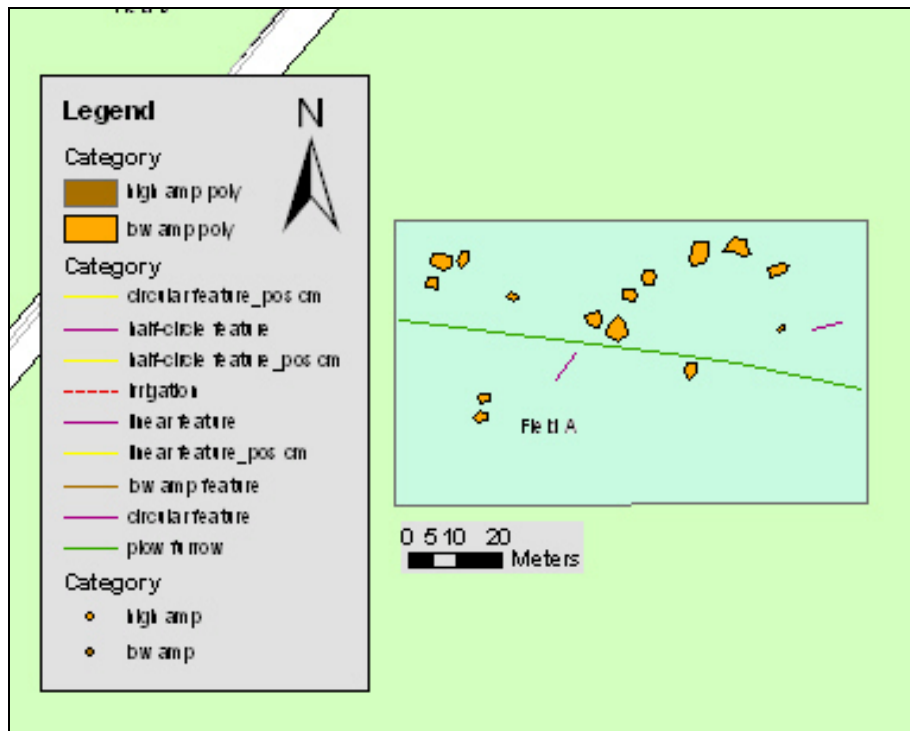


Figure 20 Field A GPR interpretations.

The high amplitude polygons may appear to be in a random order, but with the overlay of mapped crop marks, these may be anomalies remnant from the ‘woodhenge’ monument. Increased sampling of GPR data collection may better define these anomalies and provide additional information on the remaining archaeology of this monument.

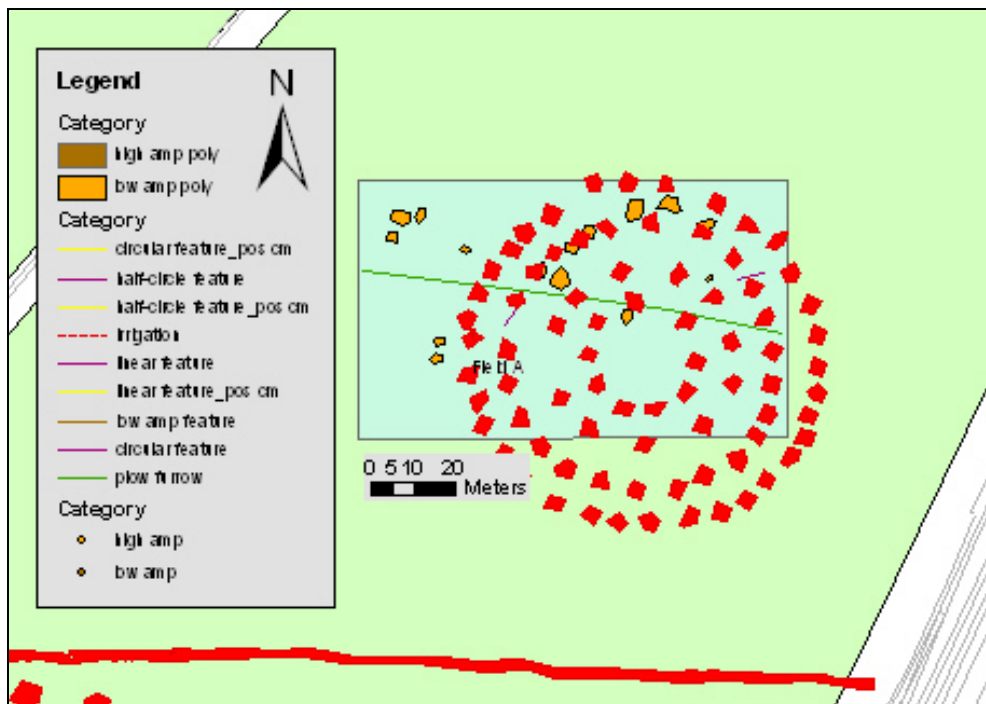
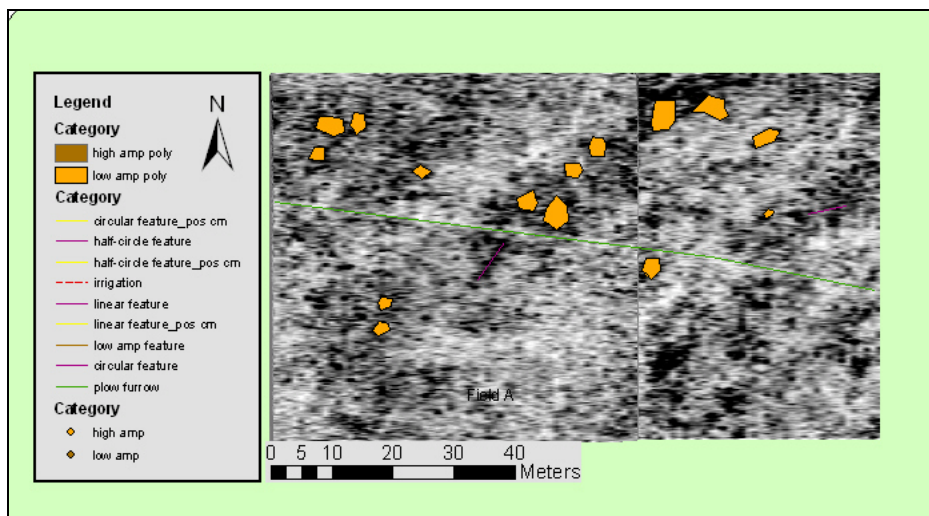
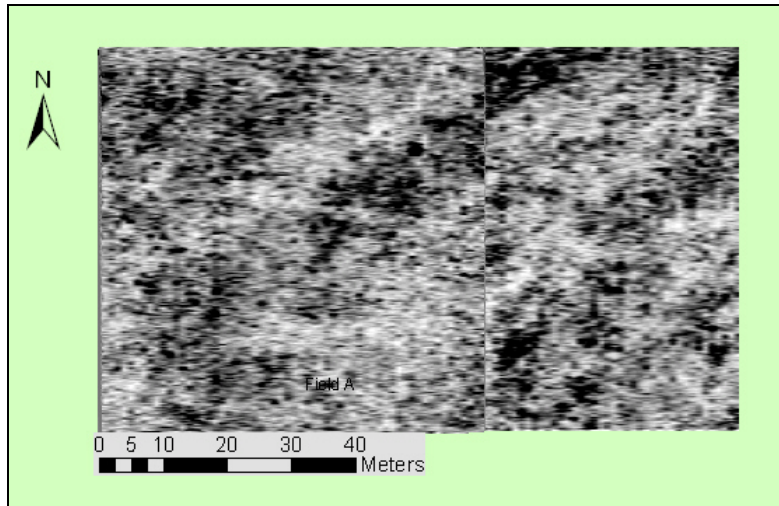


Figure 21 Field A GPR interpretations with overlain mapped crop marks.



**Figure 22 Field A GPR data (top) and data with interpretations (bottom).**

*Field B*

An 80 x 80 m grid was surveyed in field B. This grid was positioned to cover all aspects of the 'sunburst' monument including: a possible double ditch, pit alignments, a central enclosure, and some apparently 'empty' area outside of this feature.

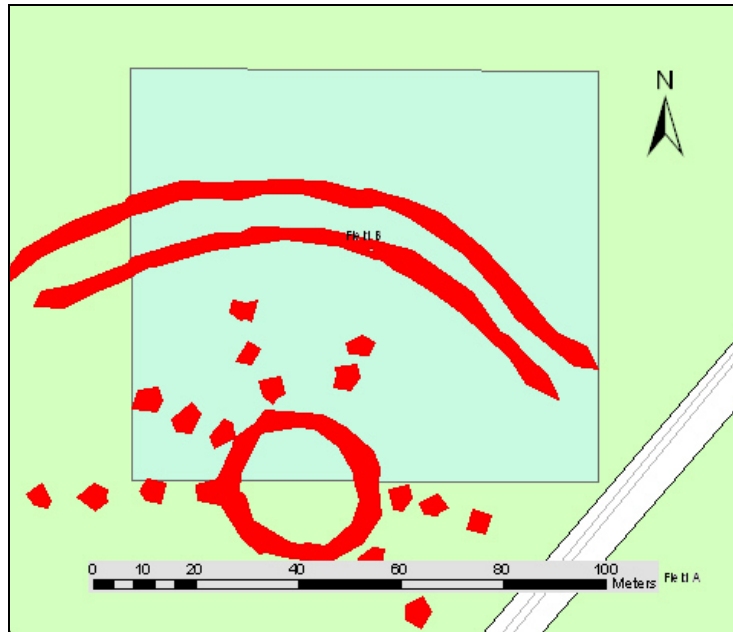


**Figure 23 Field B GPR survey Grid.**

GPR has successfully recorded traces of the archaeology over the ‘sunburst’ monument.

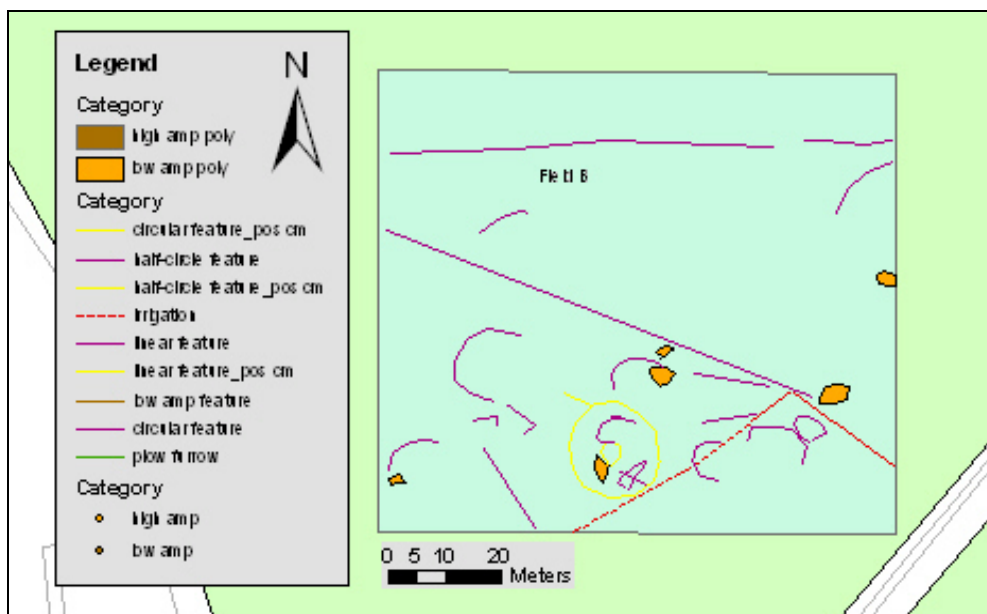


**Figure 24 Field B GPR interpretations.**

A circular anomaly with a diameter of 16 m can be clearly seen in the GPR data. The circle that defines this anomaly is a low amplitude reflector that is approximately 2 m wide. This circle has distinctive interior structure:

- A low amplitude circular anomaly is located directly in the centre of the larger circle. This interior anomaly has a diameter of approximately 3 to 3.3m;
- Linear anomalies are identified;
- Areas of high and low amplitude can also be seen.

Other than the distinctive central circle within the larger circular anomaly, more refined anomaly identification is difficult. This can be attributed to two factors: scale of data sampling (more closely spaced transects will reveal a better image) and data interpolation factors. Data that appear in this report and the GIS have undergone at least two different interpolation processes (one in RADAN, the other in ERDAS Imagine). Fine details and lines that may appear in the data may be resulting interpolation artefacts.

The two linear anomalies that span the data set from west to east (one is on a diagonal NW to SE) do not appear to be plough furrows. The diagonal anomaly appears to define an edge between high and low amplitude areas in the data, this is a broader trend that can typically be categorised as geological. Please note that the contrasting light and dark vertical band on the eastern side of the data set is an artefact from mismatched gain settings, this is not a geological or archaeological anomaly. In fact, upon close consideration, the low amplitude layer can be seen to continue into this band.

A few other half-circular anomalies can be seen in the data. These can be archaeological in nature, or perhaps remnants from ploughing or fluvial activity.

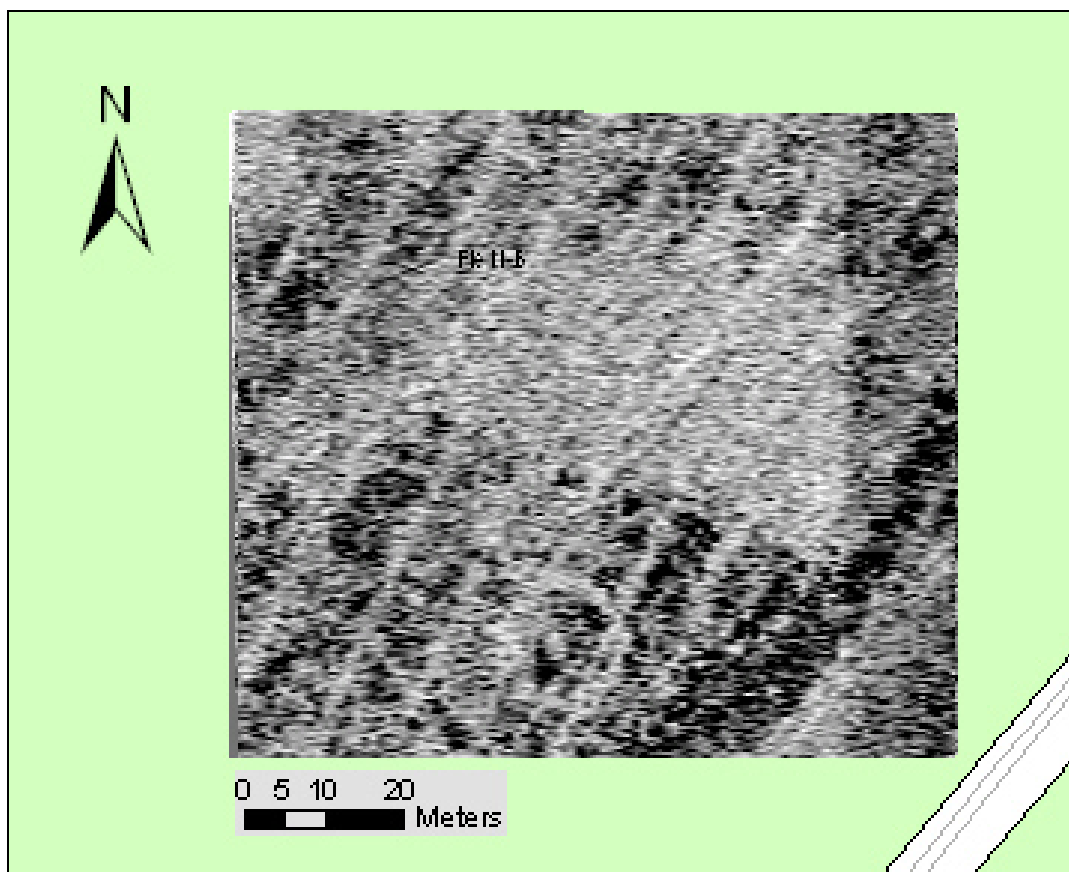


**Figure 25 Field B GPR data.**

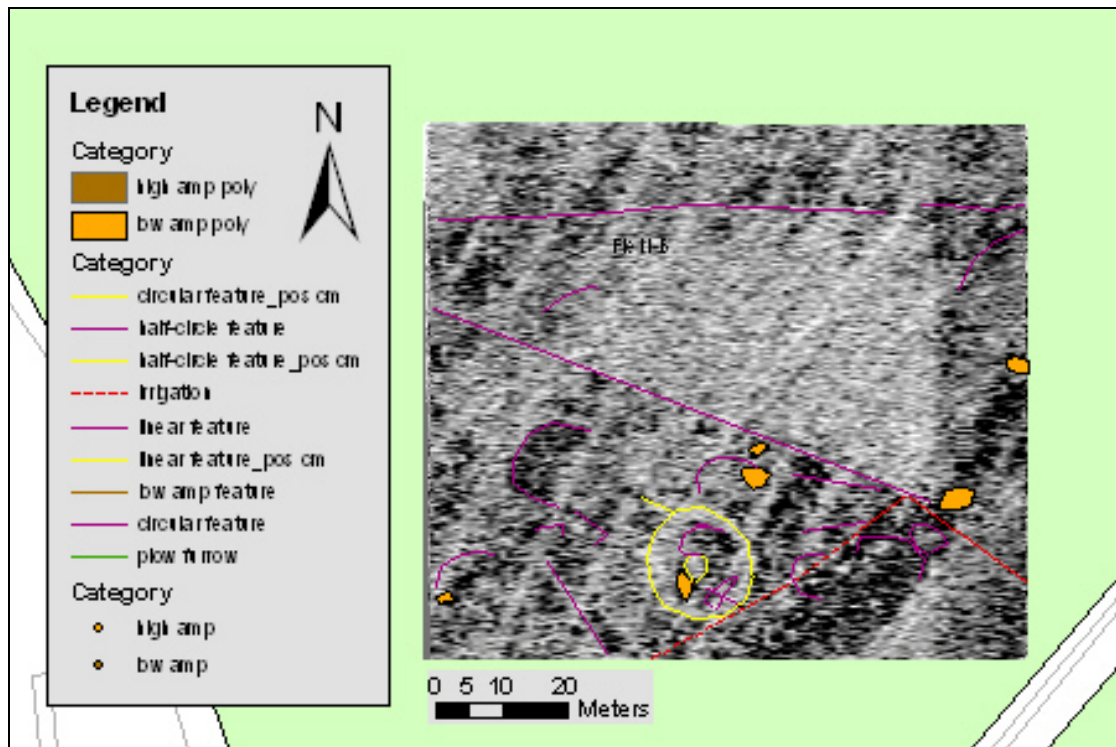


Figure 26 Field B GPR data with interpretations.



Figure 27 Field B GPR data with interpretations and mapped crop marks.

As can be seen in Figure 27, the circular anomaly in the radar data is offset from the mapped crop mark by approximately 12 to 27 m. The radiating pit alignments were not clearly mapped, although one may be appearing in the data (yellow line on the

northwest side of the circle). The possible double ditch feature encircling the ‘sunburst’ is not clearly mapped at all in the GPR data.

The offset of the crop mark feature to the actual GPR survey anomaly can be explained by scales of resolution used in mapping geophysical surveys (see above section on Methodology, Geophysical Survey Grids) and the creation of OS based crop mark maps from aerial photography interpretation (see Conclusions and Recommendations). This is a very important issue that becomes obvious when considering archaeological factors such as: area definition for SAM sites, placement of excavation trenches and other investigations.

The circular anomaly in the radar data that is identified as corresponding to the central feature of the ‘sunburst’ appears in a time slice of data that also has vestiges of previous ploughing, probably ridge and furrow. The time slices in Field B are all 7 ns. During data analysis, time slices of various thickness were considered. It is interesting to note that the anomaly does not appear at all in the data if the time slice is larger than 15 ns. The modern ploughing appears in the GPR data until approximately 7.5 ns with the crop mark appear at approximately 7.75 ns.

Thus far, the GPR data in this report has been presented as horizontal plan views to best communicate what is being found in the data. It is very important to also consider the vertical aspect of GPR data, beyond providing approximate depth to anomalies. Because of the proximity of the modern plough furrows, probable ridge and furrow features and the crop mark feature, the vertical component of GPR data cannot be ignored in order to gain better insight into what is happening in this field, as well as to the scheduled monument.

The following images are taken from RADAN and are meant to best display the order and depth of the features that are mapped in the radar data. The depth of features in the following images is estimated based on a dielectric permittivity of 30, an approximation of values determined from migration of hyperbolas across the site. The depth should not be considered real, but an approximation to be calibrated with ground truthing.

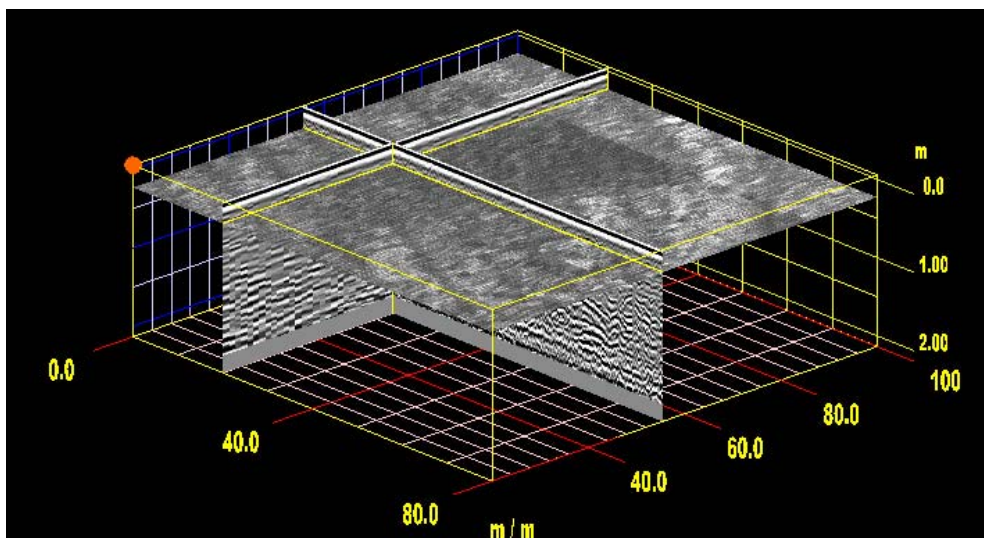


Figure 28 Field B GPR 3D cube.